

1 **High resolution decadal precipitation predictions over the**
2 **continental United States for impacts assessment**

3
4 KAUSTUBH SALVI¹, GABRIELE VILLARINI¹, GABRIEL A. VECCHI^{2*}

5
6 ¹IIHR-Hydroscience & Engineering, The University of Iowa, Iowa City, Iowa, USA

7 ²NOAA/Geophysical Fluid Dynamics Laboratory, Princeton, New Jersey, USA

8 * Current affiliation: Geosciences Department, Princeton University, Princeton, NJ, USA

9
10
11 Manuscript submitted to

12 *Journal of Hydrology*

13 Revised 6th Jun 2017

14
15
16
17 *Corresponding author:*

18 Kaustubh Salvi, IIHR-Hydroscience & Engineering, The University of Iowa, 100 C. Maxwell
19 Stanley Hydraulics Laboratory, Iowa City, 52242, Iowa, USA. E-mail: kaustubhanil-
20 salvi@uiowa.edu

24 **Abstract**

25 Unprecedented alterations in precipitation characteristics over the last century and especially in
26 the last two decades have posed serious socio-economic problems to society in terms of hydro-
27 meteorological extremes, in particular flooding and droughts. The origin of these alterations has
28 its roots in changing climatic conditions; however, its threatening implications can only be dealt
29 with through meticulous planning that is based on realistic and skillful decadal precipitation
30 predictions (DPPs). Skillful DPPs represent a very challenging prospect because of the
31 complexities associated with precipitation predictions. Because of the limited skill and coarse
32 spatial resolution, the DPPs provided by General Circulation Models (GCMs) fail to be directly
33 applicable for impact assessment. Here, we focus on nine GCMs and quantify the seasonally and
34 regionally averaged skill in DPPs over the continental United States. We address the problems
35 pertaining to the limited skill and resolution by applying linear and kernel regression-based
36 statistical downscaling approaches. For both the approaches, statistical relationships established
37 over the calibration period (1961-1990) are applied to the retrospective and near future decadal
38 predictions by GCMs to obtain DPPs at ~4km resolution. The skill is quantified across different
39 metrics that evaluate potential skill, biases, long-term statistical properties, and uncertainty. Both
40 the statistical approaches show improvements with respect to the raw GCM data, particularly in
41 terms of the long-term statistical properties and uncertainty, irrespective of lead time. The
42 outcome of the study is monthly DPPs from nine GCMs with 4-km spatial resolution, which can
43 be used as a key input for impacts assessments.

44 **Keywords:** Decadal predictions, continental United States, statistical downscaling, precipitation

45 **1. Introduction**

46 Water is the most abundant natural resource that manifests itself in diverse states and forms
47 such as precipitation, snowfall, surface and ground water, rivers, lakes, oceans. Despite such a
48 wide availability, most of our activities pertaining to water are constrained because of a lower
49 percentage of available fresh water, upcoming problems concerning water usage, and even the
50 solutions adopted to negotiate the problems. For instance, to address elevated food requirements
51 of the rising population (population more than quadrupled in 100 years), measures such as
52 doubled crop land area, six-fold increase in irrigated area (*Freydank and Siebert, 2008*) are
53 implemented, leading to rise in global water use (i.e., withdrawal) by nearly 8 times with a steep
54 increase at a rate of 15% per decade between 1960 and 2010. Such measures have put additional
55 constraints on the available fresh water resources and the exacerbating situations demand careful
56 planning and mastering of the available water resources. However, design and implementation of
57 water resources planning measures is a difficult task because precipitation represents a key input.
58 Precipitation is the most important and equally complex climate variable to understand and
59 foresee mainly because of extreme variability, revealed by precipitation patterns at different
60 spatio-temporal resolutions. The variability in precipitation might lead to high-intensity disasters
61 such as flooding and mudslides (*Trenberth et al., 2007*), or lower-intensity, longer-duration
62 events such as droughts (e.g., *Gray, 2009; Henry et al., 2004; Hunter et al., 2011*). Such
63 catastrophes not only lead to heavy infrastructure damages and pose a serious threat to life but
64 also lead to sensitive issues such as migration, which has been a common strategy to avert the
65 consequences of weather events and/or a changing climate (e.g., *Nawrotzki et al., 2012, Kniveton*
66 *et al., 2008; McLeman and Smit, 2006*).

67 The background discussed up to this point highlights the importance of precipitation and the
68 associated problems, and leads us to concluding that such problems can be mitigated only

69 through robust planning policies. The success of such measures would be highly dependent on
70 the knowledge of future precipitation, which itself represents an extremely challenging task. Our
71 current best knowledge of future precipitation and the associated uncertainties can be obtained
72 from projections from General Circulation models (GCMs) produced in support of the fifth
73 generation of Coupled Model Intercomparison Project (CMIP5) framework. This includes results
74 from a standard set of experiments by state-of-the-art climate models developed by different
75 teams of experts worldwide. This “ensemble of opportunity” (commonly used terminology to
76 represent the suite of GCM data; e.g., *Sanderson et al.*, 2015) is the best available source of
77 information on the range of physically plausible climate evolutions over the next century.
78 Representative Concentration Pathways (RCPs) from the CMIP5 suite provide us with future
79 projections of climate variables as a possible response to different radiative forcings. These
80 projections solve our problem to a certain extent and provide us with the climate projections as a
81 possible response to these forcings. However, there is a three-fold problem associated with the
82 use of GCM projections in the planning process: (1) the RCP scenarios are driven by end-
83 conditions, where the trajectories of different climate variables are plausible responses to the
84 corresponding radiative forcing at the end of the 21st century. Such projections form a better way
85 of understanding the long-term future of climate variables, but they cannot be used for short-term
86 planning policies. This is because realistic weather conditions that we encounter in our day-to-
87 day life are driven by their initial rather than their boundary conditions. Also, it is established
88 that long-term behaviors of climate variables may differ from their short term properties (e.g.,
89 *Cane*, 2010; *van Oldenborgh et al.*, 2012). (2) A complex variable such as precipitation is
90 difficult to predict and the skill exhibited by the GCM in projecting them is limited. (3) The
91 coarse spatial resolution at which the GCM projections are available cannot be used for impacts

92 assessment over limited areas. CMIP5 simulations themselves tend to resolve the first problem
93 by providing decadal scale forecasts that are initialized every year or intermittently to provide
94 predictions for the next 10-30 years. These predictions are known as decadal predictions, which
95 range from 10 to 30 year lead times (*Meehl et al., 2009*) and are forced with observed initial and
96 boundary conditions. Initialized decadal predictions, while still in their infancy, have been
97 subject to increasing attention by the scientific community. These are called upon by different
98 names, including “a new kid on the block,” “the fascinating baby that all wish to talk about”
99 (*Goddard et al., 2012*), “high profile predictions” (*Goddard et al., 2013*). Several scientists are
100 currently working on evaluating: (i) different aspects of this new product such as initialization
101 strategies (*Meehl et al., 2014*), assessment of skill in decadal predictions (*Meehl et al., 2009*),
102 gap between decadal climate predictability and predictions, impacts of initialization (*Branstator
103 and Teng, 2012*), opportunities and challenges, importance of ocean observations for successful
104 decadal predictions (*Hurrell et al., 2009*), positive phase of the inter-decadal Pacific oscillations
105 (*Meehl et al., 2016*), role of sea ice, land surface, stratosphere, and aerosols in decadal-scale
106 predictability (*Bellucci et al., 2015a*), and comparison between initialized and non-initialized
107 predictions (*Fyfe et al., 2011*); (ii) performances of individual GCM with respect to the decadal
108 predictions e.g. Flexible Global Ocean-Atmosphere-Land System model, Grid-point Version 2
109 (FGOALS-g2) (*Bin et al., 2012*), coupled Earth System model of the Max Planck Institute for
110 Meteorology (MPI-ESM) (*Muller et al., 2012*), MIROC4h and MIROC5 (*Mochizuki et al.,
111 2011*); and (iii) the skill of decadal predictions for different climate variables and quantities,
112 including surface temperature (*Smith et al., 2007; Choi et al., 2016; Salvi et al. 2017*), Sahelian
113 precipitation (*Gaetani and Mohino, 2013*), hurricane activity (*Smith et al., 2010; Vecchi et al.,
114 2013*), and regional surface climate (*Kim et al., 2012; van Oldenborgh, 2012; Doblas-Reyes et*

115 *al.*, 2013; *Goddard et al.*, 2013; *Caron et al.*, 2014; *Meehl et al.*, 2014; *Bellucci et al.*, 2015b).
116 However, despite recent progress, we still have to comprehensively quantify the quality of GCM
117 precipitation predictions, including over the United States; moreover, even though CMIP5
118 simulations have outperformed CMIP3 in terms of spatial resolution, the resolution is still not
119 high enough for impacts assessment. With this background, the goal of this work is to obtain
120 high-resolution precipitation decadal predictions over the continental United States (CONUS).

121 The specific objectives of this study involve: 1) the evaluation of raw GCM precipitation
122 skill over CONUS; 2) the enhancement of the skill using two data-driven approaches; and 3) the
123 development of a dataset of decadal predictions of precipitation over CONUS at a spatial
124 resolution of ~4 km. The two data-driven approaches that are implemented in this study are
125 transfer function based statistical downscaling (SD) methodologies. Transfer function based
126 downscaling methodologies rely upon establishing statistical relationships between coarse
127 resolution climate variables (predictors) that are relatively well understood in terms of
128 underlying physics and hence, well simulated, and the fine resolution climate variable of interest
129 that needs to be downscaled, i.e. predictand (precipitation in this study). The established
130 relationships are applied to GCM predictions to obtain downscaled data. We use two SD
131 approaches: (1) linear regression (LR) based, which assumes a parametric form of the
132 relationship, with the variation between predictors and predictand that is assumed to be linear;
133 and (2) kernel regression (KR) based, which is a non-parametric form of regression. The premise
134 behind the selection of two methodologies that are categorized under the same cluster (transfer
135 function approach) is explained in section 3. These methodologies are applied to the predictors
136 by nine GCMs to obtain improved decadal precipitation predictions at fine spatial resolution (~4
137 km). The manuscript is organized as follows. Details about the study region and the data used are

138 in Section 2. Section 3 provides details about the data-driven approaches, which are applied here
139 to enhance the prediction skills and different evaluation metrics. The results of the evaluation of
140 raw and processed GCMs' skill are discussed in Section 4. We conclude this study with
141 summary and discussion in Section 5, followed by concluding remarks.

142

143 **2. Study region and data**

144 Figure 1 shows the spatial variations of precipitation over the study region for the period
145 1961-2014, obtained using the Parameter–Elevation Regressions on Independent Slopes Model
146 (PRISM) data product (additional information about the PRISM data product can be found in
147 Section 2.1). The figure also provides the details about the seven regions we focus on: Northeast
148 (NE), Midwest (MW), Southeast (SE), Great Plains North (GPN), Great Plains South (GPS),
149 Northwest (NW), and Southwest (SW). These regional delineations are largely based on the
150 National Climate Assessment Report (*Karl et al.*, 2009) and then implemented in different
151 studies (e.g., *Pryor and Schoof*, 2008). Similar to the recent studies, which use slightly modified
152 delineations (*Schoof et al.*, 2010; *Kunkel et al.*, 2013; *Mutiibwa et al.*, 2015), we divide the Great
153 Plains into two regions GPN and GPS. The division of the Great Plains into two visually
154 homogeneous regions (homogeneous in terms of spatial variation of average precipitation) is an
155 additional advantage for the improvement in performance of SD. In this study, we focus on the
156 seven regions in Figure 1 and consider each one as an individual unit for: 1) applying statistical
157 downscaling methodologies and 2) quantifying prediction skill in regionally and seasonally
158 averaged spatio-temporal framework. Based on Figure 1, it is clear that the spatial distribution of
159 the average precipitation over CONUS shows extreme variability, in particular in areas, where
160 precipitation is mainly influenced by orography. This large spatial variability distinguishes NW

161 and SW regions from the others, where a relatively smooth transition is encountered. We
162 envision capturing the spatial variability through downscaling methodologies to prove the
163 worthiness of the downscaled precipitation for impacts assessment.

164

165 **2.1 Observed precipitation data**

166 We select PRISM precipitation dataset at monthly temporal and ~4km spatial resolution as
167 the baseline dataset. The PRISM precipitation data is used in the establishment of the statistical
168 relationships and also as the reference data for the evaluation of the decadal precipitation
169 predictions skills. PRISM (*Daly et al., 2002; Hijmans et al., 2005*) represents high-resolution
170 climate observations that are derived from a wide range of monitoring networks to illustrate
171 short- and long-term climate patterns. Point observations (precipitation measurements), obtained
172 from the monitoring networks, a digital elevation model (DEM), and other spatial datasets to
173 generate gridded estimates of annual, monthly and event-based climatic parameters (*Daly et al.,*
174 *1994*) are utilized to generate the high-resolution dataset. Here, we use the monthly PRISM
175 precipitation product from 1961 to 2014 over CONUS. There are specific limitations of the
176 dataset such as the problem with the choice of the domains for the regressions (*Widmann and*
177 *Bretherton, 1999*) and temporal discontinuities because of heterogeneous station network
178 (*UCAR, 2016*). However, the above mentioned positive features of this dataset (e.g. the high
179 spatial resolution for impacts analysis, and positive performance in regions of complex terrain)
180 make PRISM an appropriate product for our study.

181

182 **2.2 Reanalysis data**

183 We use two SD approaches to obtain high-resolution predictions. The success of the data-
184 driven approaches such as SD is highly dependent on the choice and quality of the predictors.
185 Usually, standard reanalysis data products are validated for their quality and hence, used as
186 sources of predictors. Reanalysis data are gridded data for climate variables over the entire globe,
187 derived by applying data assimilation techniques over past data, including global radiosonde
188 data, a Comprehensive Ocean-Atmosphere Data Set (COADS) that comprises a collection of
189 surface marine data, aircraft data, surface land synoptic data, satellite sounder data, Special
190 Sensing Microwave/Imager surface wind speeds, and satellite cloud drift winds. Here, we use
191 reanalysis data for establishing statistical relationships with the predictand and to remove
192 systematic errors from the GCM predictions. Different reanalysis data products are available at
193 different spatial and temporal scales, including the European Centre for Medium-Range Weather
194 Forecasts (ECMWF) reanalysis data (ERA40; *Uppala et al.*, 2005), ERA-Interim (*Dee et al.*,
195 2011), National Center for Environmental Prediction / National Center for Atmospheric
196 Research (NCEP/NCAR; *Kalnay et al.*, 1996), and the Japanese 25-year ReAnalysis (JRA-25;
197 *Onogi et al.*, 2007), and JRA-55 (*Ebita et al.*, 2011; *Kobayashi et al.*, 2015) from the Japan
198 Meteorological Agency. Statistical relationships are better established if a sufficient sample size
199 is available: NCEP/NCAR reanalysis provides longer records of reanalysis climate variable data
200 compared to other available products, with positive assets such as fixed state-of-the-art
201 assimilation scheme, inclusion of more observations, better quality control (*Bromwich and Fogt*,
202 2004), better accessibility and spatial coverage over the regions where observed data are not
203 available, and better categorization of climate variables based on the influences of observations
204 over the climate variable. ‘Categorization of climate variable’ is an important feature of this
205 product, allowing the users to identify each reanalysis climate variable with a category such as

206 ‘A’, ‘B’, and ‘C’ (Kalnay *et al.*, 1996), where category ‘A’ variables show higher accuracy
207 compared to the other ones. As mentioned before, the success of SD also relies upon the choice
208 of predictors, which represent synoptic scale circulation patterns over a study region, should be
209 well simulated by climate models and should be associated with precipitation processes (Wilby *et*
210 *al.*, 2004). The categorical distinctions of predictors in the case of NCEP/NCAR data serve as a
211 guideline to choose appropriate climate variables as predictors. Here, we consider four surface
212 level climate variables, such as mean sea level pressure (psl), temperature (tas), near surface
213 zonal (uas) wind, near surface meridional (vas) wind, and five pressure level climate variables (at
214 500hPa), including specific humidity (hus), geopotential height (zg), temperature (ta), Uwind
215 (ua), and Vwind (va). Most of the predictors that we select belong to the category ‘A’.

216

217 **2.3 GCMs used**

218 As a part of the CMIP5 program, a large number of GCMs provide the monthly decadal
219 prediction of precipitation and are initialized either each year or intermittently. We use a set of
220 nine GCMs for the analysis and Figure 2 illustrates three important details about the
221 corresponding GCM data, i.e. the name and spatial resolution, the years of initialization, and the
222 availability of the predictions based on different lead times. The lead time, which represents the
223 time lag between the year of the initialization and the year of the prediction, varies from 1 to 30
224 years. However, we restrict our analysis to the first 10 annual lead times mainly because of two
225 reasons. First, the availability of the decadal predictions for longer lead times is too small to
226 provide a conclusive estimate of skill. Secondly, the influence of initial conditions, with which
227 the models are forced, reduces with lead times (Meehl *et al.*, 2009). It is important to note that
228 the initialization patterns differ across the GCMs. Hence, we cannot get the same number of

229 GCMs contributing to the ensemble for a particular initialization. The bottom-right panel in
230 Figure 2 summarizes the number of GCMs available for each and lead time; for instance, certain
231 initializations (e.g. 1961, 1965) have their contributions from all the GCMs, whereas there is
232 only one GCM which provides the predictions that are initialized in the year 2013-2015. It is
233 clear that the presence of a higher number of GCMs provides additional confidence in the
234 predictions, which we lack for the most recent years based on the CMIP5 models.

235

236 **3. Methodology and skill assessment**

237 The SD methodologies that we use can be categorized under the broad umbrella of the
238 transfer function approaches (e.g., *Ghosh and Mujumdar, 2006; Kannan and Ghosh, 2013;*
239 *Srinivas et al, 2014*). We use LR and KR based SD models to establish statistical relationships
240 between predictors and predictand. These methodologies are applied to each season separately.
241 For both the approaches, the overall methodology remains the same. The two approaches differ
242 from each other over the models that we use to link coarse level climate variables with the fine
243 resolution predictand. The reason behind the selection of two approaches lies in the complexity
244 of the climate variable that we intend to capture (precipitation). Precipitation is a highly complex
245 climate variable and there is a possibility that different attributes of precipitations that are
246 important in the planning process such as total rainfall, seasonal variations, extremes, may not be
247 captured by a single SD approach. Hence, we use two transfer function approaches. Two datasets
248 originating from the two approaches are validated thoroughly to specify the positive attributes of
249 each product, which would help in planning. These methodologies are well established and have
250 been applied successfully, for instance, for rainfall projections with kernel regression approach
251 (e.g., *Kannan and Ghosh, 2013; Salvi et al., 2013*) and monthly rainfall projections with linear

252 regression approach (e.g., *Kannan et al.*, 2014; *Shashikanth et al.*, 2014). Here, we briefly
253 describe the specific steps that are carried out while applying the methodologies, and additional
254 details are provided in the supplementary material and in the literature (*Kannan and Ghosh*,
255 2013; *Kannan et al.*, 2014). We select 30 years (1961-1990) as calibration period and 24 years
256 (1991-2014) as validation period. We justify the selection of 1961-1990 as calibration period by
257 carrying out sensitivity analysis. We select three different time slices as calibration periods (each
258 of 30 years) and obtain the predictions for the validation period. Based on this sensitivity
259 analysis, the skills for different seasons and regions vary with calibration period and we cannot
260 identify a particular calibration period which provides the best results in all the cases. Hence, we
261 select 1961-1990 as the calibration period for this study. The details can be found in the
262 supplementary material (Sections S3, S-Figure 20). The downscaling approach begins with the
263 identification of ‘zone of predictors’ (e.g., *Salvi et al.*, 2013, 2015), which represents an
264 imaginary area (usually rectangular or square in shape) that surrounds the study region. It is
265 assumed that the predictors in the zone of predictors influence the precipitation in the
266 corresponding region. Because we work with seven regions, we have seven zones of predictors.
267 S-Figures 1-9 show the spatial extent of each zone of predictors, obtained using a correlation
268 analysis approach (e.g., *Kannan and Ghosh*, 2010; *Salvi et al.*, 2013). After the selection of the
269 zone of the predictors, we proceed to the establishment of the statistical relationship between
270 reanalysis climate variables over the zone of predictor and individual precipitation at each pixel
271 in the region. To deal with the multicollinearity (i.e., correlation among predictors) and
272 multidimensionality, we select and apply principal component analysis (PCA) as a
273 dimensionality reduction technique. PCA is a form of orthogonal transformation that converts
274 the correlated predictors into non-correlated principal components (PC) and arranges them in

275 descending order of variability explained by each one. There is no single criterion about the
276 selection of the number of PCs which would need to be retained in establishing the statistical
277 relationship. A number of methods have been proposed in the literature to select the number of
278 PCs, including the selection of PCs with eigen value greater than unity (*Kaiser*, 1960), Akaike
279 information criterion (*Akaike*, 1974), cumulative percent variance (*Malinowski*, 1991), and
280 variance of the reconstruction error (*Qin*, 1998; *Valle et al.*, 1999). In this study, we mainly use
281 the “percentage of variance explained” criterion to select the number of PCs, which involves the
282 selection of the first few PCs for model calibration/validation depending upon the desired level
283 of variability retained. As the 30-year calibration period provides us with a sample size of 90 (30
284 years \times 3 months per season), we select the first three PCs of each predictor, leading to a total of
285 27 PCs (9 predictors \times 3 PCs). For LR, we put an additional filter over these 27 PCs and select
286 only those PCs (out of 27) which show a statistically significant relationship with the observed
287 precipitation at each pixel. S-Figure 10 shows that on average between 3 and 10 PCs in a 95%
288 confidence interval are used to establish the statistical relationship after the application of the
289 second filter. The established statistical relationship is assumed to be time-invariant and applied
290 to obtain: 1) precipitation with NCEP/NCAR reanalysis data for the validation period, and 2)
291 decadal scale climate predictions with bias corrected GCM predictions. The details about the
292 methodology can be found in the supplementary material (Sections S1-2).

293 Three sets of results (i.e., ensemble raw GCM predictions and ensemble GCM predictions
294 after statistical downscaling with both the approaches) are evaluated with respect to different
295 metrics. The performance of raw GCM predictions and the downscaled precipitations (with LR
296 and KR) are evaluated over the validation period (1991-2014). These assessments are carried out
297 over ‘lead-wise’ seasonally and regionally averaged time series for both the raw and the

298 downscaled precipitation and we refer to this as the ‘spatio-temporally averaged framework.’
 299 The regional delineations in Figure 1 are used to obtain spatially averaged time series to
 300 represent the respective regions. To obtain seasonal averages, we choose four seasons: spring
 301 (MAM), summer (JJA), fall (SON), and winter (DJF) and the complete year (YEAR). This
 302 results in the representative time series with 24 data points (one representative value for each
 303 season over the validation period of 24 years). This is different from some of the studies (*Singh*
 304 *et al.*, 2012; *Gaetani and Mohino*, 2013; *Tiwari et al.*, 2014), which retained monthly values
 305 even in the seasonal time series, resulting in 72 data points for each season (24 years \times 3 months
 306 per year): one of the major limitations of such approach is the enhanced correlation due to the
 307 capturing of the seasonality of precipitation (e.g., November is wetter than October which is also
 308 wetter than September) rather than the correct values, potentially leading to an erroneous
 309 impression about the skill possessed by the predictions. Hence, we retain the prior validation
 310 approach (one representative value per region per season per year). This approach provides a
 311 much more direct information about the skill of the models (whether the raw GCM or after the
 312 statistical downscaling) for each season without having to rely on the climatology to achieve
 313 good skill. The evaluation of regionally and seasonally averaged time series is carried out
 314 considering three metrics. Each metric represents a specific quality that we intend to quantify for
 315 decadal predictions. The first metric represents a linear association between observation and
 316 predictions known as skill score (SS). *Murphy and Winkler* (1992) proposed a decomposed
 317 version of the skill score in terms of potential skill and biases (conditional and unconditional) as
 318 shown in equation 1:

$$SS = \rho_{fx}^2 - \left[\rho_{fx} - \left(\frac{\sigma_f}{\sigma_x} \right) \right]^2 - \left[\frac{(\mu_f - \mu_x)}{\sigma_x} \right]^2 \quad (1)$$

319 where, ρ_{fx} is the correlation between predictions and observations; σ_f and σ_x are the standard
320 deviation, while μ_f and μ_x are the mean of the predictions and the observations, respectively. The
321 first term of the decomposition (right-hand side) is the potential skill (PS) of the forecasts
322 without any bias. The second term is known as the slope reliability (SREL) and is a measure of
323 the conditional bias. The third term is a standardized mean error (SME), a measure of the
324 unconditional bias (*Hashino et al., 2007*). We refer to this correlation-based metric as “Memory-
325 based” metric (*Dirmeyer et al., 2016*). The second metric represents the skill pertaining to the
326 long term statistical properties such as mean, standard deviation (STDEV), extremes (95th
327 percentile), and root mean square error (RMSE), which we refer to as “Long-term statistics
328 based” metrics. The third metric represents the quantification and visual assessment of inter-
329 model uncertainty, obtained in terms of the envelope of nine GCM predictions, and we refer to
330 this as “Uncertainty-based” metric. We also compare the statistically downscaled GCM
331 predictions with both approaches on a decadal scale as well: instead of comparing the predictions
332 lead-wise for 1991-2014, we compare them decade-wise e.g. 1961-1970, 1961-1971. This is the
333 format in which GCMs provide the data and our motive in comparing the two products in this
334 manner is to identify the skill metrics which retain the consistency across different initializations.
335 We call this comparison as “decadal framework” and we make these comparisons for regionally
336 averaged time series (one time series for each region with 12 months \times 10 years = 120 data
337 points).

338
339
340
341

342 **4. Results**

343 **4.1 Skill of the raw GCMs' predictions**

344 Regionally and seasonally averaged raw GCM precipitation predictions (ensemble) for
345 different lead times (in years, from 1 to 10) are evaluated for Memory-based and Long-term
346 statistics metrics and the results are presented in Figure 3. Overall, GCM predictions are
347 characterized by low PS values, ranging from 0 to 0.3. For most of the lead times, the PS values
348 are as low as 0.1. For different regions, patches of slightly elevated PS values are encountered
349 (e.g., GPS, NE, SW at the yearly scale; GPS, MW, NE, SE, SW in winter; NW in spring; NE,
350 SW in summer; MW, NW in fall). Surprisingly, the higher PS values do not always correspond
351 to the lead-1 predictions. This finding is contradictory to our pre-conceived belief that smaller
352 differences between initialization and year of prediction should provide the best results,
353 assuming the highest influence of initial conditions for shorter lead times. The absence of
354 conditional bias, revealed in terms of lower SREL values, is the only positive aspect of the raw
355 GCM predictions. This is consistent for all regions and seasons and across all lead times.
356 However, the presence of unconditional bias in terms of higher SME values for most of the
357 regions brings down the overall skills (SS). This is mainly visible for GPN, SW (over all
358 seasons), MW and NE over winter and SE over summer. As a result, the values of the actual skill
359 SS turn negative in magnitude. The fall season lacks unconditional biases and hence, positive SS
360 are observed for GPS, MW, NE, and NW for certain lead times. Raw GCM predictions do not
361 fare well when compared with observed precipitation based on long term statistical properties.
362 The comparison of statistical properties, expressed as absolute difference between ensemble
363 predictions and PRISM data, shows high differences for all the statistical properties for almost
364 all regions and seasons over different lead times. In fact, high difference in mean and standard

365 deviations is the prime cause for higher unconditional biases (SME) leading to poor skill. Except
366 for the fall season, large differences in mean indicate that the GCMs lack the capability to
367 capture the total amount of precipitation, and large differences in STDEV indicate their failure to
368 capture the variability. Equally small skill values are revealed for extremes and RMSE, except
369 for the extremes at the yearly temporal scale, where raw GCM predictions can reproduce the
370 observations reasonably well. This analysis confirms the statement that usually GCM predictions
371 for a climate variable such as precipitation cannot be directly used because they possess low
372 skills.

373

374 **4.2 Uncertainty quantification for the raw GCM predictions**

375 The nine GCMs enable us to assess and quantify the uncertainty in precipitation predictions
376 (Figure 4). These envelopes can be considered as a surrogate for the uncertainty in GCMs. Here,
377 we discuss the results for lead-1, while the details about other lead times are shown in the
378 supplementary material (S-Figures 11-19). All the plots show a wide uncertainty envelope (gray
379 envelope) indicating that different GCM predictions, averaged over different seasons and regions
380 differ from each other significantly. Along with the envelope, we compare the ensemble time
381 series (shown by the blue line) with the observed data. Most of the regions show deviations
382 between the ensemble time series and the observed precipitation data, representing biases in the
383 predictions. One prominent feature of the observed data is high variability, which is indicated by
384 large fluctuations (e.g. NE region in spring and summer). Ensemble raw GCM predictions fail to
385 capture the variability present in the observed precipitation time series. The results in Figures 3-4
386 show that the skills pertaining to the original GCM predictions are mediocre across the different

387 evaluation metrics used here, with limited potential skill, large unconditional biases and
388 uncertainty.

389 Bias correction techniques, such as ‘Bias Correction and Spatial Disaggregation’ (BCSD) (Wood
390 et al., 2004) and ‘Quantile mapping method’ (Li et al., 2010), have been extensively used in the
391 literature to obtain skillful rainfall projections. However, it is important to understand that the
392 removal of the bias requires the correction of the statistical properties/quantiles of GCMs
393 projections to match the cumulative distribution function (CDF) of the observed data over
394 historic (calibration) period at each pixel. It is obvious that these methods would result in “bias-
395 free” projections with respect to the historical period; however, they cannot add any skill on their
396 own unless the raw GCM projections are skillful. Therefore, the inherent skill in the GCM
397 predictions represents a prerequisite for the application of such bias correction methods: bias
398 correction methodologies should be used only for those climate variables that are reasonably
399 well simulated by the GCMs otherwise it might lead to unrealistic predictions. Based on the
400 results in Figure 3, the raw GCMs do not possess the skills to predict precipitation. Also, the bias
401 correction does not involve any regional level modelling. Therefore, we choose two downscaling
402 approaches (LR and KR based SD) in the present study, which involve regional level modelling,
403 and our expectation is that the obtained data are more realistic. The subsequent sections provide
404 the details of the methodical validations and the skill-evaluation exercise of the downscaled
405 precipitation.

406

407 **4.3 Validation of the downscaling models**

408 Figure 5 shows the results of the validation based on Memory-based and Long-term statistics
409 for the LR and KR-statistically downscaled products that are obtained with NCEP/NCAR

410 forcings over the validation period (1991-2014). As discussed in section 3, the validations are
411 illustrated in the spatio-temporally averaged framework for each season and region. Downscaled
412 precipitation with LR shows better Memory-based skills as compared to KR. This is clear from
413 the PS plots over different regions, where PS for LR approach are higher than those for KR for
414 most of the seasons and regions. High PS values (above 0.5 leading to values of the correlation
415 coefficient larger than 0.7) are found for all the regions, except for NE over different seasons.
416 The methodology shows a very good performance for such a highly complex variable to predict.
417 The LR is capable of removing the conditional (SREL) and unconditional biases (SME) for all
418 the regions and seasons, resulting in positive values of SS. In fact, there are hardly any losses in
419 the skill because of the presence of biases. The KR methodology shows a comparable
420 performance in removing the biases. However, this model is not able to capture the season-to-
421 season variations in the observed data, resulting in lower values of PS as compared to the LR.
422 This is reflected in SS as well, where the KR shows negative SS for some cases (e.g., yearly SS
423 for GPN, MW). The second set of validation metrics (i.e. Long-term statistics based validations)
424 shows a complete reversal of skill. The comparison over variability, expressed in terms of
425 absolute differences in standard deviation and extremes clearly shows that the KR model
426 outperforms LR. The two models reveal similar skill when compared with respect to the absolute
427 difference in mean and RMSE. Overall, the validation results highlight the capability of the two
428 SD models in capturing some important properties of observed precipitation (i.e., the LR
429 captures the season-to-season variability and mean, while the KR captures long term variability
430 and extremes). The specific skill shown by the two methodologies can be an important guideline
431 in selecting the downscaled product for a particular study or application.

432 Having established the credibility of downscaling models with the reanalysis forcings, we
433 move ahead with the evaluation of the decadal prediction skills for precipitation obtained with
434 the GCM forcings. Before building the statistical relationships with respect to the nine
435 predictors, we assess the skills of the GCM forcings. We have carried out a separate analysis for
436 each one of them (refer to section S4 of the supplementary material) and found out that the
437 decadal predictions of the predictors are reasonably good compared to the raw precipitation skills
438 (Figure 3), and can be included as predictors in the SD models.

439

440 **4.4 Evaluation of the LR-based GCM predictions**

441 Figure 6 shows the Memory-based and Long-term statistics based skill-evaluation plots for
442 the precipitation downscaled with LR at the regionally and seasonally averaged scale. Compared
443 to the raw GCM predictions, we do not see significant improvements in PS. We do, though,
444 observed instances of relatively high PS across all seasons and for different regions. Similar to
445 the raw predictions, these instances do not follow the influences of initial conditions and hence,
446 in some cases, higher skill is observed at long lead times (e.g., NE in summer for lead period 7-
447 8). As far as conditional and unconditional biases are concerned, there are marked improvements
448 with respect to the raw predictions, especially for SME. The LR model is able to reduce the
449 impact of these biases, resulting in positive SS. Overall, positive skill is observed mainly for the
450 winter and spring seasons. The predictions obtained with LR show better linear association with
451 the PRISM data as compared to its raw counterpart. The best part of the downscaled precipitation
452 with LR is the skills with which the long term mean is captured. For most of the regions and
453 seasons, the absolute difference between observed data and predictions is small (~5-7
454 mm/month). The same methodology fails to perform at the same level in capturing other long

455 term statistical properties, such as variations in terms of STDEV, extremes and RMSE, leading
456 to no significant improvements as compared to the raw predictions. Pixel-wise skills for
457 downscaled precipitation, obtained by applying LR based downscaling approach for different
458 lead times from 1 to 10 (years) in the form of US maps are shown in the supplementary material
459 (from S-Figure 21 to S-Figure 30).

460

461 **4.5 Uncertainty quantification for LR-based GCM predictions**

462 The LR methodology showed the capability in closing the gap between PRISM and GCM
463 predictions with respect to the mean precipitation. Here, we assess the improvements with
464 respect to the uncertainty-based metrics, focusing on the results corresponding to the lead-1
465 (Figure 7), while those for the other lead times are shown in the supplementary material (S-
466 Figures 31-39). The results for all regions and seasons lead us to two critical improvements in
467 the LR based downscaled product as compared to the raw GCM predictions. The first
468 improvement is in terms of reduced uncertainty. This is evident from the GCM envelopes (gray
469 bands), which are considerably smaller than the raw predictions (Figure 4). The second
470 improvement is the reduction in the gap between observed time series (black line) and ensemble
471 mean predictions (blue line). This gap represents biases in the predictions and here it is
472 completely eliminated (e.g., compare the uncertainty envelope for GPN in Figure 4 and Figure
473 7). Along with these improvements, Figure 7 brings out some of the shortcomings of the LR
474 approach as well. For all regions and seasons, the blue line, representing the ensemble of all
475 GCM predictions, is able to trace the mean trajectory of the PRISM data, even though it
476 completely fails to capture the large fluctuations. As far as uncertainty-based metrics are

477 concerned, they are the exact replica of the validation shown in Figure 6, where the long term
478 mean is captured with a high accuracy and the fluctuations are too small.

479

480 **4.6 Evaluation of the KR-based GCM predictions**

481 We evaluate the skill of the decadal precipitation predictions obtained using the KR approach
482 and present the results in Figure 8. The KR approach is able to slightly increase the values of PS
483 in the predictions, even though these increases are small compared to the raw GCM predictions.
484 For most of the regions and seasons, the PS is around 0.15, and the higher skills are not
485 necessarily for the 1-year lead. One such example is SW region, which shows higher PS at
486 different lead times (lead-7 for yearly, lead-8 for winter) other than lead-1. The real enhancement
487 in the downscaled product is observed in the complete removal of conditional and unconditional
488 biases. The effect of this suppression is visualized in SS, where positive residual skill is present
489 for different lead times. Positive values of SS represent an indirect indication that the KR
490 approach shows the credibility to retain one-to-one association between the downscaled GCM
491 product and PRISM precipitation at least for some of the lead times. This is mainly observed for
492 the regions: MW, NW, SE, SW (at the yearly scale), GPN, MW, NE, SE, SW (over winter);
493 GPN, MW, NE, SW (over spring); GPN, GPS, MW, NE, NW, SW (over summer); and GPS,
494 MW, NE, NW, SE (over fall). The second positive attribute of KR approach is its ability to
495 capture long term statistical properties, especially the mean. The approach shows good skill in
496 capturing the long term mean (Figure 8), with the absolute difference between observed
497 precipitation and GCM predictions that is about ~5 mm/month. Similar to the skill displayed by
498 LR, the KR approach is not able to capture either the standard deviation, extreme and RMSE,
499 except for the yearly scale. For other seasons, we observe cases in which the methodology

500 captured STDEV and EXTREMES with excellent skills (e.g., SW in summer and fall; GPN in
501 year and winter). Pixel-wise skills for downscaled precipitation, obtained by applying KR based
502 downscaling approach for different lead times from 1 to 10 in the form of U.S. maps are shown
503 in the supplementary material (from S-Figure 40 to S-Figure 49).

504

505 **4.7 Uncertainty quantification for KR-based GCM predictions**

506 We evaluate the downscaled precipitation with the KR approach in terms of GCM envelopes
507 (Figure 9). Similar to the prior assessments (Figures 4 and 7), we restrict our discussion to lead-1
508 predictions only, with the evaluations for the other lead times in the supplementary material (S-
509 Figures 50-58). Overall, here are two positive attributes associated with the KR, similar to what
510 is discussed for LR. There is reduced uncertainty as shown by the reduction in the width of the
511 GCM envelopes (gray band) as compared to the raw predictions in Figure 4. Also, ensemble
512 GCM predictions (blue line) runs through the central tendency of the PRISM precipitation (black
513 line), eliminating the biases between the two. The methodology is therefore able to capture the
514 long term mean but not the fluctuations, similar to what was discussed for the LR methodology.
515 If we compare the two downscaled products, we find that the LR approach performs better in
516 reducing the uncertainty as compared to the KR methodology, evident from the width of the
517 GCM envelope that is smaller. However, the ensemble GCM predictions for the downscaled
518 precipitation with LR show little or no fluctuations at all, while those with the KR approach
519 shows slightly higher degree of year-to-year variability.

520

521 **4.8 Further validations of decadal predictions**

522 In the previous sections (4.1-4.7), we provided a thorough evaluation of the raw GCM
523 predictions and the statistically downscaled products obtained with the LR and KR. The focus of
524 the validation was on the assessment of the prediction skill in a seasonally and regionally
525 averaged spatio-temporal framework, for lead times from one to ten years. Such a lead-wise
526 quantification of skill was possible because of the availability of several retrospective
527 predictions, which enabled us to construct lead-wise datasets for validation. However, GCM
528 predictions are not provided in a lead-wise format. Hence, the spatio-temporally averaged
529 framework validation approach considered in this study cannot be used to assess GCM
530 predictions in the form of single initialization of ‘ten-year predictions’ (decade). Here we modify
531 the validation approach to be tailored to single initializations. We obtain regionally averaged
532 time series of decadal predictions, consisting of 120 values (12 months \times 10 years = 120 values)
533 and compare them with the PRISM data to evaluate their performance. The motivation behind
534 this type of evaluations lies in the fact that the decadal predictions are initialized either yearly or
535 intermittently to provide the predictions for ten years. Therefore, we may not get the advantage
536 of data availability to evaluate lead-wise skills. This procedure is carried out for each
537 initialization (e.g., there are nine GCMs that are initialized with respect to the observations for
538 the year 1961 to provide the predictions for 1961-1970). We obtain the ensemble of these nine
539 GCMs and generate a regionally averaged times series (120 values) and estimate the skill by
540 comparing the time series with regionally averaged PRISM observations for 1961-1970. The
541 number of GCM predictions available at different initializations differs based on the data
542 availability (e.g., for the predictions initialized in 1962 only five GCMs are available and we use
543 just those five for obtaining the ensemble mean). A similar step is repeated for predictions that
544 are initialized from 1961 onwards until 2005. We stop at the initialization year 2005 because the

545 validation period for the present study is restricted to 2014 (which is the last year for the decadal
546 predictions that are initialized in 2005). We evaluate the skill of decadal predictions using three
547 metrics: 1) PS (representing the one-to-one association between predictions and PRISM data), 2)
548 absolute percentage difference in mean (representing the total precipitation over a decade), and
549 3) absolute percentage difference in extremes (95th percentile, representing difference in
550 extremes). We evaluate both data products (with LR and KR) and the results of this analysis are
551 illustrated in Figure 10 in terms of radar plots. Each plot consists of 45 spokes, each representing
552 a single decade (e.g., 1961-1970, 1962-1971) and labeled with the year in which the predictions
553 was initialized. For regions GPN, MW, and NW there is high PS and the performance is
554 consistent over all the decades, irrespective of the calibration/validation period. Both the
555 downscaled precipitation products show similar PS, indicating that the methodologies are able to
556 capture the one-to-one association over the mentioned region with a high confidence. GPS shows
557 reasonable skills over the training period, even though the values of PS decline over the testing
558 period. Both the downscaled products perform poorly over the regions NE, SE, and SW. The
559 LR- and KR-SD precipitation predictions fare well in terms of capturing long term mean,
560 represented in terms of absolute percentage difference and expressed as a fraction. GPN, MW,
561 and SE are the regions where both the products show excellent skill in capturing observed mean
562 (maximum difference smaller than 8%). Over the other regions, this difference is restricted to
563 less than 15%, which makes these products a viable input data for impact studies. As far as PS
564 and mean are concerned, the performance of both products is comparable. The real differences
565 manifest themselves when we focus on the extremes. For all the regions, the extremes are better
566 captured with the KR methodology. For most of the regions, the differences for KR based
567 predictions are about 30%.

568

569 **4.9 Decadal predictions up to 2024**

570 Here we present future precipitation predictions over 2015-2024 (Figure 11). We use lead-
571 10 data to ensure maximum future coverage. Each plot shows possible future variations in
572 seasonally and regionally averaged precipitation obtained with the LR and KR approaches, with
573 reference to the past baseline precipitation (average precipitation of 1981-2010) for a particular
574 season and region. There are certain common features shared by almost all the plots. Ensemble
575 future predictions (for both products) do not show a strong trend, indicating lack of variations in
576 average precipitation. Also, these predictions are close to the baseline precipitation implying
577 almost no change in future precipitation predictions as compared to the past. Future predictions
578 with both the downscaled products are along a comparable trajectory. However, these statements
579 are valid until 2022. We observe certain erratic behavior for the years post 2022. Also, the ‘in-
580 sync’ behavior between the two data products until 2022 fades away for the last three years and
581 we encounter differences between the two. However, this behavior can be attributed to the lack
582 of predictions over these years. We just have a single GCM (CanCM4), which provides the data
583 until 2015, significantly decreasing our confidence in the predictions after 2022. Also, as
584 previously discussed, the predictions follow the trajectory, tracing the mean of the observed data
585 but lack the variability in the observations. Assuming the same pattern to manifest in the future,
586 it is expected to have much larger variability as compared to what is being depicted in the figure.

587

588

589 **5. Discussion and conclusions**

590 This study evaluates and enhances the skill of initialized decadal precipitation predictions
591 over the continental United States (CONUS) and generate high resolution (~4km) precipitation
592 prediction products by applying statistical downscaling (SD) methodologies. The downscaled
593 precipitation products that are obtained with Linear Regression (LR) and Kernel Regression
594 (KR) approaches are evaluated by imposing a stringent validation framework to understand the
595 positive/negative attributes of these predictions. Raw General Circulation Models (GCM)
596 predictions, when evaluated over different metrics, showed lack of skill (SS) because of the
597 presence of high biases and high uncertainties, indicating that GCM predictions differ from one
598 another, resulting in wide envelopes. Hence, it can be concluded that raw GCM predictions
599 cannot be directly used for impacts assessments studies.

600 The validation of LR and KR models is performed to assess the credibility of two SD
601 approaches over downscaled precipitation data, obtained with NCEP/NCAR forcings. Results
602 show the strength of both the SD models in capturing some of the important properties of the
603 observed precipitation. LR model shows superiority in capturing seasonal variations for most of
604 the regions, showing positive residual skill (Skills Score) thank to the reduction in biases. On the
605 other hand, the KR model captures the long term variability (standard deviations, extremes).
606 These differences in performance support our need for the use of two SD approaches that can be
607 categorized under the transfer function approach. The validation results serve as guidelines in
608 selecting the data product based on the study that one intends to carry out: for instance, to study
609 seasonal variations and formulate the policies for the same, LR-precipitation data are slightly
610 more reliable and KR-precipitation data can be used to study extremes. Both methodologies,
611 however, are capable of capturing a complex property of the observed data such as the spatial
612 variability due to orography. Figure 12 shows the comparison of mean precipitation over

613 different seasons (as discussed in section 3), obtained from the PRISM data and the statistically
614 downscaled products (both with LR and KR) with the reanalysis forcings over the testing period
615 (1991-2014). These methodologies are capable of capturing the complex spatial patterns of mean
616 precipitation, especially near the U.S. West Coast. The credibility of the methodology to capture
617 the spatial variability is extremely important from the point of view of impact assessment. This is
618 because, even though we assess the skill of the predictions in a spatio-temporally averaged
619 framework, impact assessment studies often demand reasonable skill over a much finer
620 resolution within a region of interest. At such a small scale, the local effects like orography play
621 an important role in controlling the spatial variability. Hence, a methodology that captures such
622 local effects is likely to produce skillful downscaled products suitable for impact assessment
623 studies.

624 The skill revealed by the downscaled GCM predictions is generally independent of lead
625 times. This conclusion holds against the preconceived notion that smaller lags between
626 initialization and predictions (smaller lead times) lead to higher skill. It is difficult to explain this
627 inconsistent behavior. It can be only argued that the GCMs used for predictions might suffer
628 from the shock of the initial conditions and hence, require some time before the model converges
629 to provide better result. However, this statement is just a hypothesis and assessing its validity/
630 falsifiability is out of the scope of the present study. Both the approaches show reasonable skill
631 in capturing important properties of the observed data. Similar to the skill revealed by SD
632 predictions with NCEP/NCAR data, the GCM precipitation predictions with the LR approach
633 show better skill in terms of PS and mean, whereas those with the KR approach show better skill
634 with long term variability and extremes. The marked reduction in uncertainty as indicated by the
635 reduction in the width of the GCM envelope is an indication that the downscaled precipitation

636 data from different GCMs bear a close resemblance with each other. The comparison of the two
637 products in a decadal validation framework shows that the downscaled precipitation with the
638 KR-approach appears to capture the climatology better when compared to that with LR-
639 approach. Future precipitation predictions, however, do not show a significant trend. The lack of
640 visually significant trends in future precipitation can be taken as a word of caution. This is an
641 indication that we need robust planning policies to cater to the increasing water demands,
642 especially after having understood that the total precipitation is not likely to change significantly
643 over the next few years.

644 Having discussed all the positive features of the methodology and downscaled data, we want
645 to highlight some of the limitations of the present study as well. The methodology starts with the
646 identification of zone of predictors for each of the seven regions. The seven regions are formed
647 by merging few states and they do not necessarily represent meteorologically homogeneous
648 regions. This may result in reducing some of the skill of the downscaled precipitation. The
649 assumption of stationarity is a common limitation for all data driven approaches, where the
650 statistical relationship is assumed to be time invariant. However, as we are applying the
651 relationship which is established in the near past (1961-1990), there is a fair chance that the
652 violation of the assumption will not negatively affect the results. The variability possessed by the
653 observed precipitation is generally not captured by our methodologies. This is evident from the
654 narrowness of the GCM envelopes. The accuracy with which the predictions are able to capture
655 the mean does not hold for variability and extremes. Hence, we have high confidence in the total
656 amount of precipitations that the products predict. However, the seasonal variations and
657 extremes, revealed by the downscaled precipitation should be considered with care.

658

659 *Acknowledgments*

660 This work is funded in part by the Broad Agency Announcement (BAA) Program and the
661 Engineer Research and Development Center (ERDC)–Cold Regions Research and Engineering
662 Laboratory (CRREL) under Contract No. W913E5-16-C-0002. We thank the Associate Editor,
663 Dr. Pegram and an anonymous reviewer for their comments and suggestions.

664

665 **References**

- 666 Akaike, H. (1974), Information theory and an extension of the maximum likelihood principle. In
667 Proceedings 2nd International Symposium on Information Theory; Petrov and Caski, Eds.,
668 pp 267-281.
- 669 Bellucci, A., and Co-authors (2015a), Advancements in decadal climate predictability: The role
670 of nonoceanic drivers, *Rev. Geophys.*, 53, doi:10.1002/2014RG000473.
- 671 Bellucci, A., and Co-authors (2015b), An assessment of a multi-model ensemble of decadal
672 climate predictions. *Climate Dyn.* 2787–2806, doi:10.1007/s00382-014-2164-y.
- 673 Bin, W., and Co-authors (2012), Preliminary Evaluations of FGOALS-g2 for Decadal
674 Predictions. *Advances in Atmospheric Sciences*, VOL. 30, NO. 3, 2013, 674–683.
- 675 Branstator, G., and H. Teng (2012), Potential impact of initialization on decadal predictions as
676 assessed for CMIP5 models, *Geophys. Res. Lett.*, 39, L12703, doi:10.1029/2012GL051974.
- 677 Bromwich, D. H., and R. L. Fogt (2004), Strong trends in the skill of the ERA-40 and NCEP-
678 NCAR reanalyses in the high and middle latitudes of the Southern Hemisphere, 1958 – 2001,
679 *J. Clim.*, 17, 4603 – 4619
- 680 Cane, M. (2010), Climate science: Decadal predictions in demand, *Nature Geoscience* 3, 231 -
681 232 (2010), doi:10.1038/ngeo823
- 682 Caron, L. P., C. G. Jones, F., and Doblas-Reyes (2014), Multi-year prediction skill of Atlantic
683 hurricane activity in CMIP5 decadal hindcasts. *Climate Dyn.*, 42, 2675–2690, doi:10.1007/
684 s00382-013-1773-1.
- 685 Choi, J., S. W. Son, Y. Ham, J. Lee, and H. Kim (2016), Seasonal-to-Interannual Prediction
686 Skills of Near-Surface Air Temperature in the CMIP5 Decadal Hindcast Experiments,
687 Seasonal-to-Interannual Prediction Skills of Near-Surface Air Temperature in the CMIP5
688 Decadal Hindcast Experiments. *J. Climate*, 29, 1511–1527.
- 689 Daly, C., R. P. Neilson, and D. L. Phillips (1994), A statistical-topographic model for mapping
690 climatological precipitation over mountainous terrain. *J. Appl. Meteor.*, 33, 140-158.
- 691 Daly, C., W. P. Gibson, G. H. Taylor, G. L. Johnson, and P. Pasteris (2002), A knowledge-based
692 approach to the statistical mapping of climate. *Climate Research* 22: 99–113.
- 693 Dee, D. P., and Co-authors (2011), The ERA-Interim reanalysis: configuration and performance
694 of the data assimilation system, *Q. J. Roy. Meteor. Soc.*, 137(656), 553-597
- 695 Dirmeyer, P. A., and Co-authors (2016), Confronting Weather and Climate Models with
696 Observational Data from Soil Moisture Networks over the United States, *J. Hydrometeor.*,
697 DOI: 10.1175/JHM-D-15-0196.1
- 698 Doblas-Reyes F. J., and Co-authors (2013), Initialized near-term regional climate change
699 prediction. *Nat. Commun.*, 4, 1715, doi:10.1038/ncomms2704.
- 700 Ebita, A., and Co-authors (2011), The Japanese 55-year Reanalysis “JRA-55”: An Interim report,
701 *Sola*, 7, 149–152, doi:10.2151/sola.2011-038

702 Freydanck, K., and S. Siebert (2008), Towards mapping the extent of irrigation in the last century:
703 Time series of irrigated area per country, Frankfurt Hydrol. Pap. 08, Inst. of Phys. Geogr.,
704 Univ. of Frankfurt, Frankfurt am Main, Germany.

705 Fyfe J. C., W. J. Merryfield, V. Kharin, G. J. Boer, W. S. Lee, and K. von Salzen (2011), Skillful
706 predictions of decadal trends in global mean surface temperature. *Geophys. Res. Lett.*, 38,
707 L22801, doi:10.1029/2011GL049508

708 Gaetani, M., and E. Mohino (2013), Decadal Prediction of the Sahelian Precipitation in CMIP5
709 Simulations, *Journal of Climate*, volume 26, DOI: 10.1175/JCLI-D-12-00635.1

710 Ghosh, S., and P. P. Mujumdar (2006), Future rainfall scenario over Orissa with GCM
711 projections by statistical downscaling. *Current*, 90(3).

712 Goddard, L., J. W. Hurrell, B. P. Kirtman, J. Murphy, T. Stockdale, and C. Vera (2012), Two
713 time scales for the price of one (almost). *Bull Amer Meteor Soc* 93:621–629.
714 doi:10.1175/BAMS-D-11-00220.1

715 Goddard L, and Co-authors (2013), A verification framework for interannual-to-decadal
716 predictions experiments, *Clim. Dyn.*, 40(1–2), 245–272, doi:10.1007/ s00382-012-1481-2

717 Gray, C. L. (2009), Environment, land, and rural out-migration in the southern Ecuadorian
718 Andes. *World Development*, 37(2), 457–468.

719 Hashino T, A. A. Bradley, and S. S. Schwartz (2007), Evaluation of bias-correction methods for
720 ensemble streamflow volume forecasts, *Hydrol. Earth Syst. Sci.*, 11, 939–950, 2007

721 Henry, S., B. Schoumaker, and C. Beauchemin (2004), The impact of rainfall on the first out-
722 migration: A multi-level event-history analysis in Burkina Faso. *Population and*
723 *Environment*, 25(5), 423–460.

724 Hijmans, R. J., S. E. Cameron, J. L. Parra, P. G. Jones, and A. Jarvis (2005), Very High
725 Resolution Interpolated Climate Surfaces for Global Land Areas, *International Journal of*
726 *Climatology*, *Int. J. Climatol.* 25: 1965–1978.

727 Hunter, L. M., S. Murray, and F. Riosmena (2011), Climatic variability and U.S. migration from
728 rural Mexico. Boulder: University of Colorado, Institute of Behavioral Sciences.

729 Hurrell, J. W., and Co-authors (2009), "Decadal Climate Prediction: Opportunities and
730 Challenges" in *Proceedings of OceanObs'09: Sustained Ocean Observations and Information*
731 *for Society (Vol. 2)*, Venice, Italy, 21-25 September 2009, Hall, J., Harrison, D.E. &
732 Stammer, D., Eds., ESA Publication WPP-306, doi:10.5270/OceanObs09.cwp.45

733 Kaiser, H. F. (1960), The application of electronic computers to factor analysis. *Educational and*
734 *Psychological Measurement*, 20, 141-151.

735 Kalnay, E., and Co-authors (1996), The NCEP/NCAR 40-years reanalysis project, *Bull. Am.*
736 *Meteor. Soc.*, 77(3), 437-471.

737 Kannan, S., and S. Ghosh (2010), Prediction of daily rainfall state in a river basin using statistical
738 downscaling from GCM output., *Stochastic Environmental Research and Risk Assessment*,
739 Springer.

- 740 Kannan, S., and S. Ghosh (2013), A nonparametric kernel regression model for downscaling
741 multisite daily precipitation in the Mahanadi basin, *Water Resour. Res.*, 49, 1360-1385,
742 doi:10.1002/wrcr.20118.
- 743 Kannan, S., S. Ghosh, V. Mishra, and K. Salvi (2014), Uncertainty Resulting from Multiple Data
744 Usage in Statistical Downscaling, *Geophysical Research Letter*, 41, 4013–4019,
745 DOI:10.1002/2014GL060089
- 746 Karl, T. R., J. M. Melillo, and T.C. Peterson (2009), *Global Climate Change Impacts in the*
747 *United States*. Cambridge University Press.
- 748 Kim, H-M., P. J. Webster, and J. A. Curry (2012), Evaluation of short-term climate change
749 prediction in multi-model CMIP5 decadal hindcasts. *Geophys. Res. Lett.*, 39, L10701,
750 doi:10.1029/2012GL051644.
- 751 Kniveton, D., K. Schmidt-Verkerk, C. Smith, and R. Black (2008), *Climate change and*
752 *migration: Improving methodologies to estimate flows*. Brighton: International Organization
753 for Migration.
- 754 Kobayashi, S., and Co-authors (2015), The JRA-55 reanalysis: general specifications and basic
755 characteristics. *Journal of the Meteorological Society of Japan* 93: 5–48,
756 doi:10.2151/jmsj.2015-001.
- 757 Kunkel, K. E., and Co-authors (2013), Monitoring and understanding changes in extreme storms:
758 State of knowledge, *Bull. Am. Meteorol. Soc.*, doi:10.1175/BAMS-D-12-00066.1, in press.
- 759 Li, H., J. Sheffield, and E. F. Wood (2010), Bias correction of monthly precipitation and
760 temperature fields from intergovernmental panel on climate change ar4 models using
761 equidistant quantile matching, *J. Geophys. Res.*, 115, D10101, doi:10.1029/2009JD012882.
- 762 Malinowski, E. R. (1991), *Factor Analysis in Chemistry*; Wiley-Interscience: New York.
- 763 McLeman, R., and B. Smit (2006), Migration as an adaptation to climate change. *Climatic*
764 *Change*, 76(1–2), 31–53.
- 765 Meehl, J. A., and Co-authors (2009), DECADAL PREDICTION Can It Be Skillful? *Bull. Amer.*
766 *Meteor. Soc.*, 90, 1467–1485.
- 767 Meehl, J. A., and Co-authors (2014), Decadal climate prediction: An update from the trenches.
768 *Bull. Amer. Meteor. Soc.*, 95, 243–267, doi:10.1175/BAMS-D-12-00241.1.
- 769 Meehl, G. A., A. Hu, J. M. Arblaster, J. Fasullo, and K. E. Trenberth (2016), Externally Forced
770 and Internally Generated Decadal Climate Variability Associated with the Interdecadal
771 Pacific Oscillation, *Journal of Climate*, DOI: 10.1175/JCLI-D-12-00548.1
- 772 Mochizuki, T., Y. Chikamoto, M. Kimoto, M. Ishii, H. Tatebe, Y. Komuro, and T. T. Sakamoto
773 (2011), NOTES AND CORRESPONDENCE Decadal Prediction Using a Recent Series of
774 MIROC Global Climate Models, *Journal of the Meteorological Society of Japan*, Vol. 90A,
775 pp. 373--383, 2012. 373 DOI:10.2151/jmsj.2012-A22
- 776 Müller, W. A., J. Baehr, H. Haak, J. H. Jungclaus, J. Kröger, D. Matei, D. Notz, H. Pohlmann, J.
777 S. von Storch, and J. Marotzke (2012), Forecast skill of multi-year seasonal means in the

778 decadal prediction system of the Max Planck Institute for Meteorology, *Geophys. Res. Lett.*,
779 39, L22707, doi:10.1029/2012GL053326.

780 Murphy, A. H., and R. L. Winkler (1992), Diagnostic verification of probability forecasts, *Int. J.*
781 *Forecasting*, 7, 435–455.

782 Mutiibwa, D., S. J. Vavrus, S. A. McAfee, and T. P. Albright (2015), Recent spatiotemporal
783 patterns in temperature extremes across conterminous United States. *J. Geophys. Res.*
784 *Atmos.*, 120, doi:10.1002/2015JD023598.

785 Nawrotzki, R. J., R. Riosmena, and L. M. Hunter (2013), Do Rainfall Deficits Predict U.S.-
786 Bound Migration from Rural Mexico? Evidence from the Mexican Census, *Popul Res Policy*
787 *Rev* (2013) 32:129–158, DOI 10.1007/s11113-012-9251-8

788 Onogi, K., and Co-authors (2007), The JRA-25 Reanalysis. *J. Meteor. Soc. Japan*, 85, 369-432.

789 Pryor, S. C., and J. T. Schoof (2008), Changes in the seasonality of precipitation over the
790 contiguous USA. *J. Geophys. Res.*, 113, D21108, doi:10.1029/2008JD010251.

791 Qin, S. J. (1998), Dunia, R. Determining the number of principal components for best
792 reconstruction. In IFAC DYCOPS'98, Greece.

793 Salvi, K., S. Kannan, and S. Ghosh (2013), High-resolution multisite daily rainfall projections in
794 India with statistical downscaling for climate change impacts assessment, *J. Geophys. Res.*
795 *Atmos.*, 118, 3557-3578, DOI:10.1002/jgrd.50280

796 Salvi, K., S. Ghosh, and A. R. Ganguly (2015), Credibility of Statistical Downscaling under
797 Nonstationary Climate, *Climate Dynamics*, doi: 10.1007/s00382-015-2688-9

798 Salvi, K., G. Villarini, G.A. Vecchi, and S. Ghosh, Decadal temperature predictions over the
799 continental United States: Analysis and enhancement, *Climate Dynamics*,
800 doi:10.1007/s00382-017-3532-1, 2017.

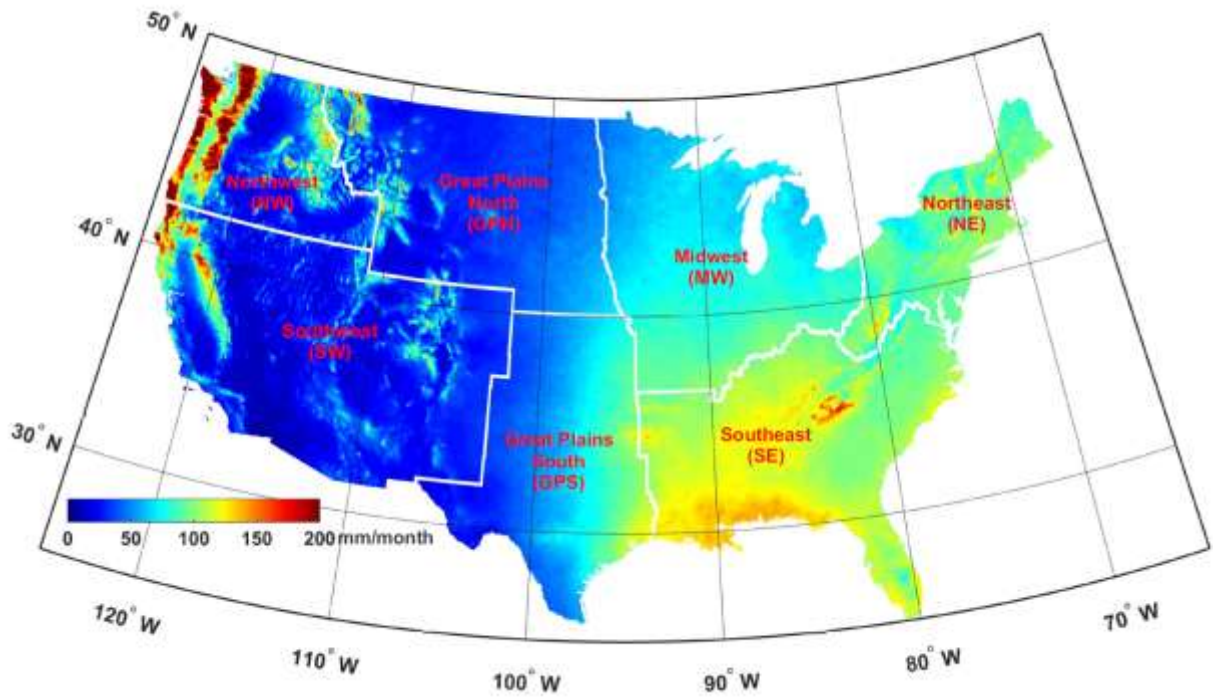
801 Sanderson, M. G., and Co-authors (2008), A multi-model source-receptor study of the
802 hemispheric transport and deposition of oxidised nitrogen, *Geophys. Res. Lett.*, 35, L17815,
803 doi:10.1029/2008GL035389, 2008.

804 Schoof, J. T., S. C. Pryor, and J. Surprenant (2010), Development of daily precipitation
805 projections for the United States based on probabilistic downscaling, *J. Geophys. Res.*, 115,
806 D13106, doi:10.1029/2009JD013030.

807 Shashikanth, K., C. G. Madhusoodhanan, S. Ghosh, T. I. Eldho, K. Rajendran, and R.
808 Murtugudde (2014), Comparing Statistically Downscaled Simulations of Indian Monsoon at
809 different spatial Resolutions, *Journal of Hydrology*, Volume 519, Part D, Pages 3163:3177,
810 10.1016/j.jhydrol.2014.10.042

811 Singh, A., M. A. Kulkarni, U. C. Mohanty, S. C. Kar, A. W. Robertson, and G. Mishra (2012),
812 Prediction of Indian summer monsoon rainfall (ISMR) using canonical correlation analysis
813 of global circulation model products *Meteorol. Appl.* 19: 179–188, DOI: 10.1002/met.1333

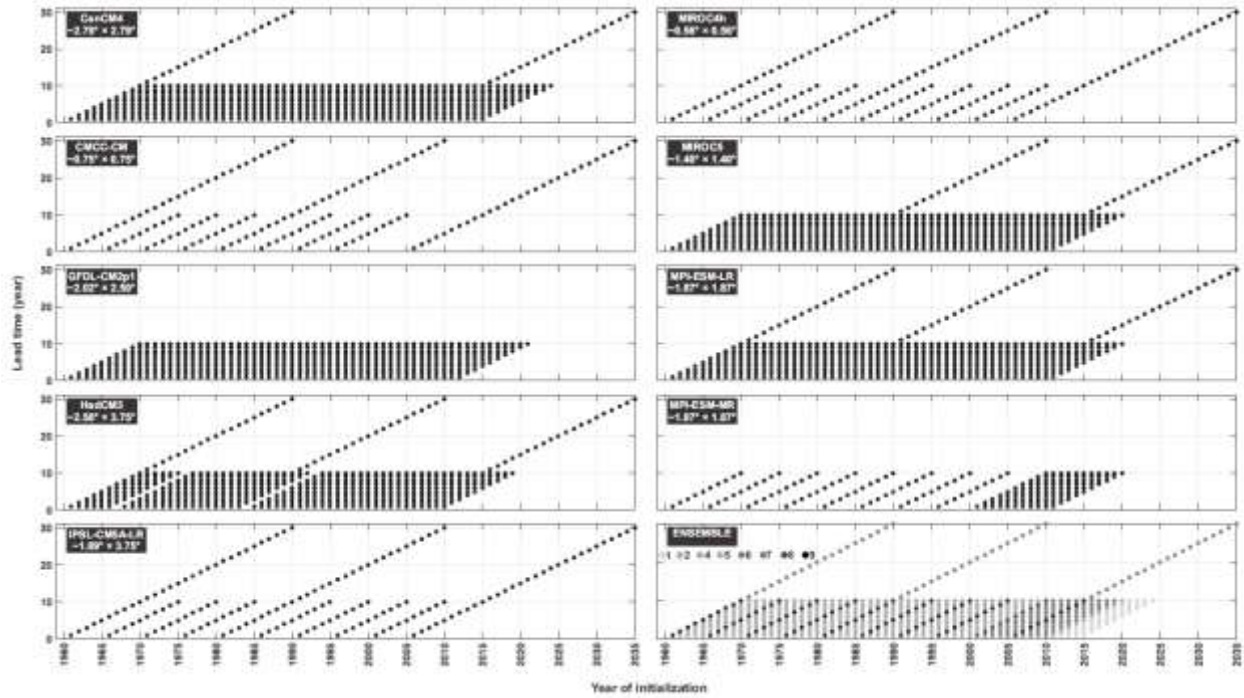
- 814 Smith, D. M., S. Cusack, A. W. Colman, C. K. Folland, G. R. Harris, and J. M. Murphy (2007),
815 Improved surface temperature prediction for the coming decade from a global climate model.
816 *Science*, 317, 796–799, doi:10.1126/science.1139540.
- 817 Smith, D. M., R. Eade, N. J. Dunstone, D. Fereday, J. M. Murphy, H. Pohlmann, and A. A.
818 Scaife (2010), Skillful multi-year predictions of Atlantic hurricane frequency. *Nat. Geosci.*,
819 3, 846–849, doi:10.1038/ngeo1004.
- 820 Srinivas, V. V., B. Basu, D. N. Kumar, and S. K. Jain (2014), Multi-site downscaling of
821 maximum and minimum daily temperature using support vector machine, *Int. J. Climatol.* 34:
822 1538–1560 (2014), DOI: 10.1002/joc.3782
- 823 Tiwari, P. R., S. C. Kar, U. C. Mohanty, S. Kumari, P. Sinha, A. Nair, and S. Dey (2014), Skill
824 of precipitation prediction with GCMs over north India during winter season *Int. J. Climatol.*
825 (2014) DOI: 10.1002/joc.3921
- 826 Trenberth, K. E., and Co-authors (2007). Observations: Surface and atmospheric climate change.
827 In S. Solomon, D. Qin, M. Manning, Z. Chen, M. Marquis, K. B. Averyt, M. Tignor, & H. L.
828 Miller (Eds.), *Climate change 2007: The physical science basis. Contribution of Working*
829 *Group I to the fourth assessment report of the Intergovernmental Panel on Climate Change.*
830 New York: Cambridge University Press.
- 831 UCAR 2016, [https://climatedataguide.ucar.edu/climate-data/prism-high-resolution-spatial-](https://climatedataguide.ucar.edu/climate-data/prism-high-resolution-spatial-climate-data-united-states-maxmin-temp-dewpoint)
832 [climate-data-united-states-maxmin-temp-dewpoint](https://climatedataguide.ucar.edu/climate-data/prism-high-resolution-spatial-climate-data-united-states-maxmin-temp-dewpoint), 25th February 2016, 10 AM
- 833 Uppala, S. M., and Co-authors (2005), The ERA-40 re-analysis. *Quart. J. R. Meteorol. Soc.*, 131,
834 29613012.doi:10.1256/qj.04.176
- 835 Valle, S., W. Li, and S. Joe Qin (1999), Selection of the Number of Principal Components: The
836 Variance of the Reconstruction Error Criterion with a Comparison to Other Methods, *Ind.*
837 *Eng. Chem. Res.* 1999, 38, 4389-4401.
- 838 van Oldenborgh, G. J., F. J. Doblas-Reyes, B. Wouters, and W. Hazeleger (2012), Skill in the
839 trend and internal variability in a multi-model decadal prediction ensemble, *Clim. Dyn.*, 38.7
840 (2012): 1263-1280.
- 841 Vecchi, G. A., and Co-authors (2013), Multi-year predictions of North Atlantic hurricane
842 frequency: Promise and limitations, *Journal of Climate*, 26(15), 5337-5357, 2013.
- 843 Widmann, M., and C. S. Bretherton (1999), Validation of Mesoscale Precipitation in the NCEP
844 Reanalysis Using a New Gridcell Dataset for the Northwestern United States, *J. Climate*, 13,
845 1936–1950. doi: [http://dx.doi.org/10.1175/1520-0442\(2000\)013<1936:VOMPIT>2.0.CO;2](http://dx.doi.org/10.1175/1520-0442(2000)013<1936:VOMPIT>2.0.CO;2)
- 846 Wilby, R. L., and Co-authors (2004), The guidelines for use of climate scenarios developed from
847 statistical downscaling methods. Supporting material of the Intergovernmental Panel on
848 Climate Change (IPCC), Prepared on behalf of Task Group on Data and Scenario Support for
849 Impacts and Climate Analysis (TGICA). ([http://ipccddc.cru.uea.ac.uk/guidelines/](http://ipccddc.cru.uea.ac.uk/guidelines/StatDownGuide.pdf)
850 [StatDownGuide.pdf](http://ipccddc.cru.uea.ac.uk/guidelines/StatDownGuide.pdf))
- 851 Wood, A. W., L. R. Leung, V. Sridhar, and D. Lettenmaier (2004), Hydrologic implications of
852 dynamical and statistical approaches to downscaling climate model outputs, *Clim. Change*,
853 62(1–3), 189–216.



855

856 Figure 1: Map showing the monthly averaged precipitation for the 1961-2014 period based on
857 the PRISM data. The map also shows the seven regions considered in the analyses.

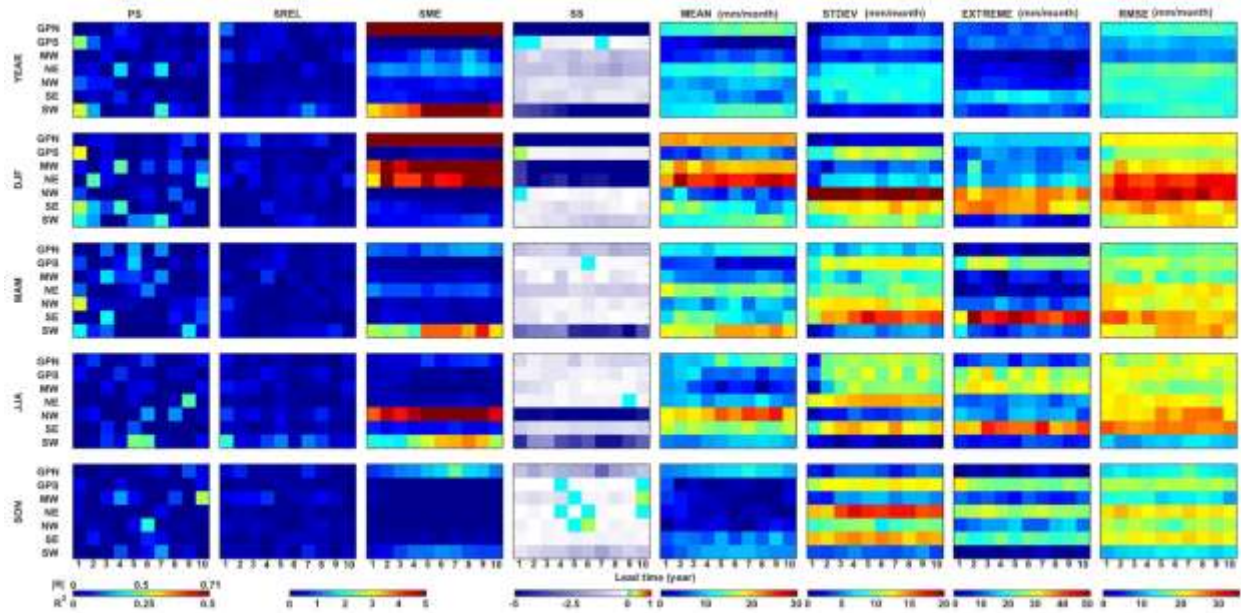
858



859

860 Figure 2: Graphical data inventory plots, illustrating the year of initialization and lead-wise
 861 prediction availability for nine GCMs along with their spatial resolution, mentioned in the top
 862 left corner of each plot. ‘Ensemble’ plot shows the number of GCMs available for different
 863 initializations and lead times for obtaining ensemble mean and uncertainty.

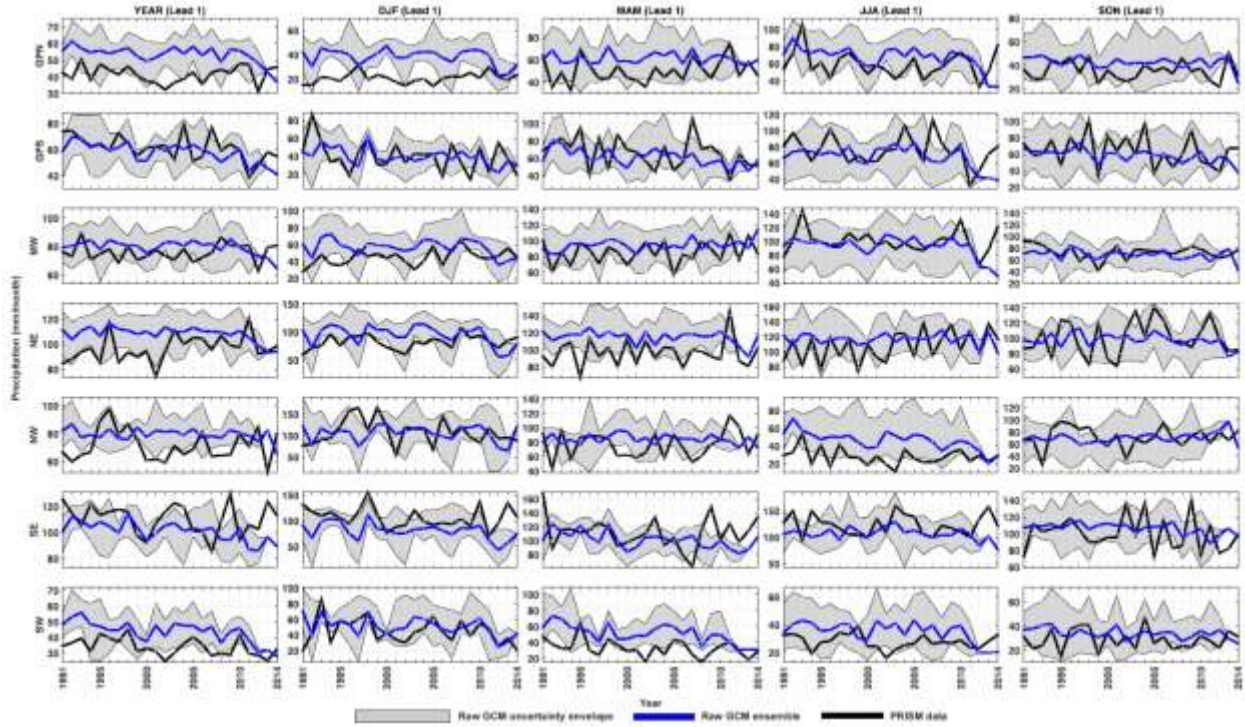
864



865

866 Figure 3: ‘Memory-based’ and ‘Long-term statistics based’ skill metrics for seasonally and
 867 regionally averaged ensembles of *raw* GCM predictions over lead times 1-10. The results are for
 868 the average of all available GCMs.

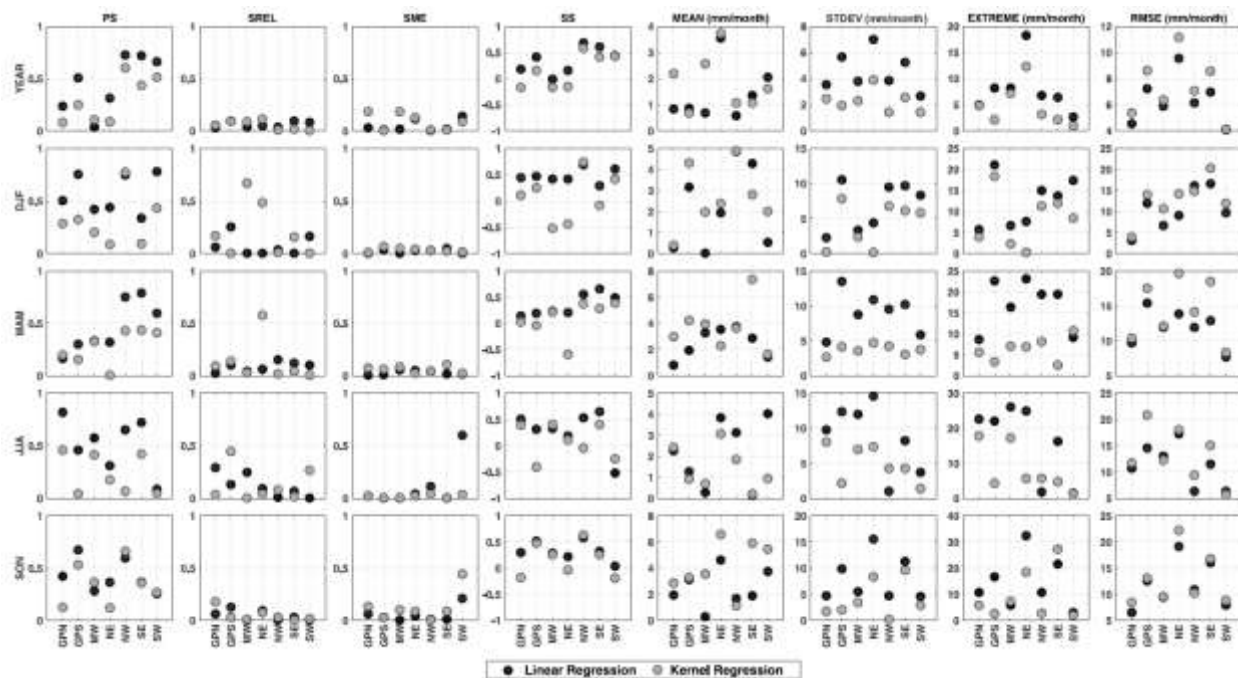
869



870

871 Figure 4: ‘Uncertainty-based’ skill metrics in terms of seasonally and regionally averaged
 872 envelope as a measure of uncertainty, obtained with 1-year lead time predictions. Wide
 873 envelopes (gray band) and high deviations of the ensemble GCM predictions (blue line) with
 874 respect to observed time series (black line) for some of the regions imply poor performance by
 875 the GCMs.

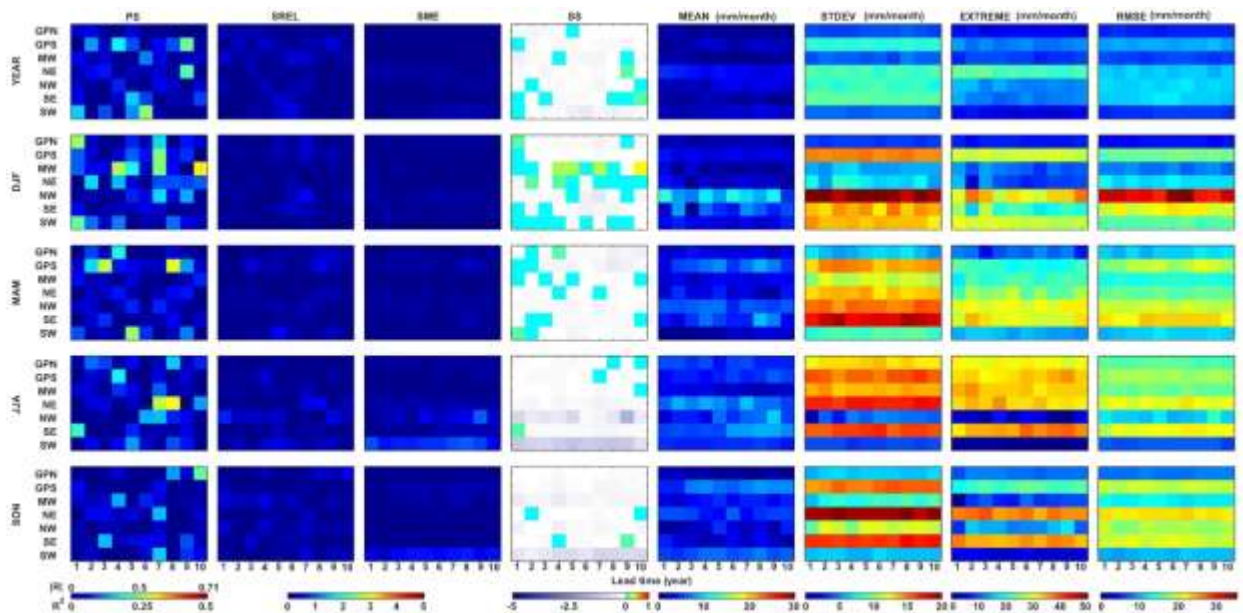
876



877

878 Figure 5: ‘Memory-based’ and ‘Long-term statistics based’ skill validations of LR and KR based
 879 SD methodologies applied to NCEP/NCAR reanalysis predictors over 1991-2014. The
 880 downscaling methodologies show increasing skill in extracting the relationship between
 881 NCEP/NCAR predictors and PRISM precipitation, evident from the positive values of SS,
 882 extremely low biases, and lower differences in long term statistical properties.

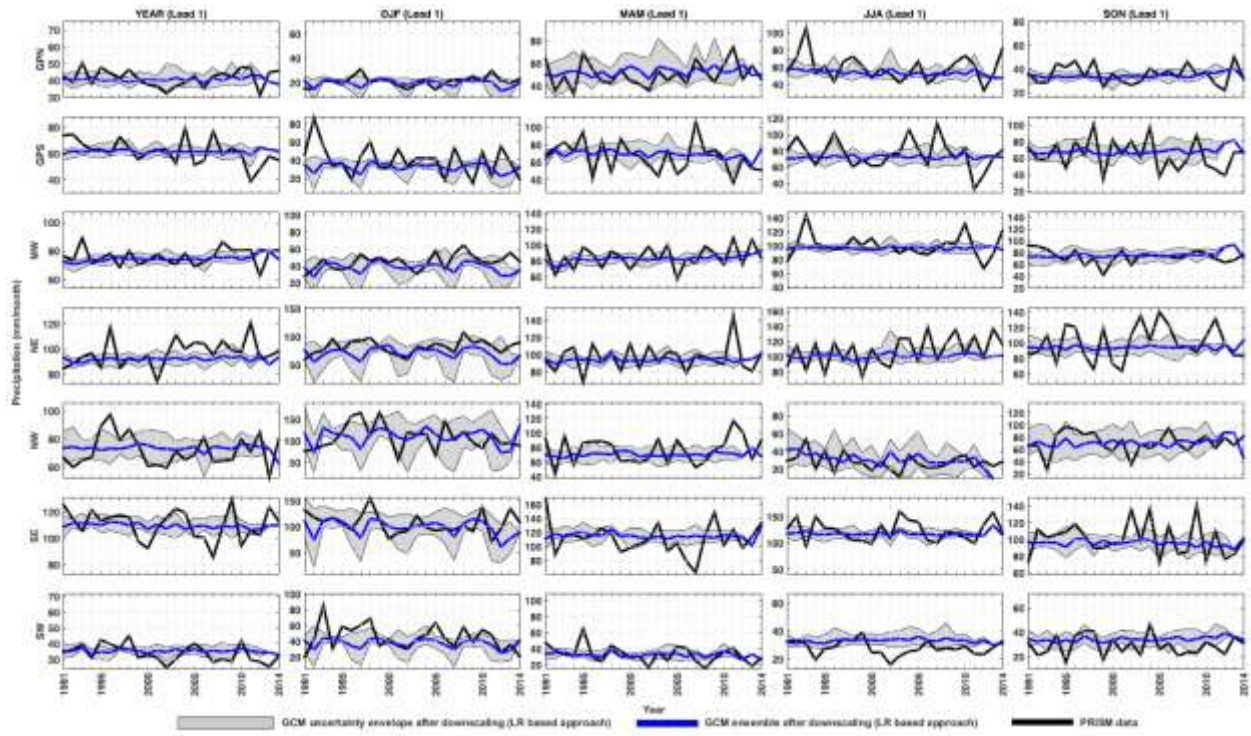
883



884

885 Figure 6: Same as Figure 3 but for seasonally and regionally averaged ensembles of LR based
 886 *statistically downscaled* GCM predictions.

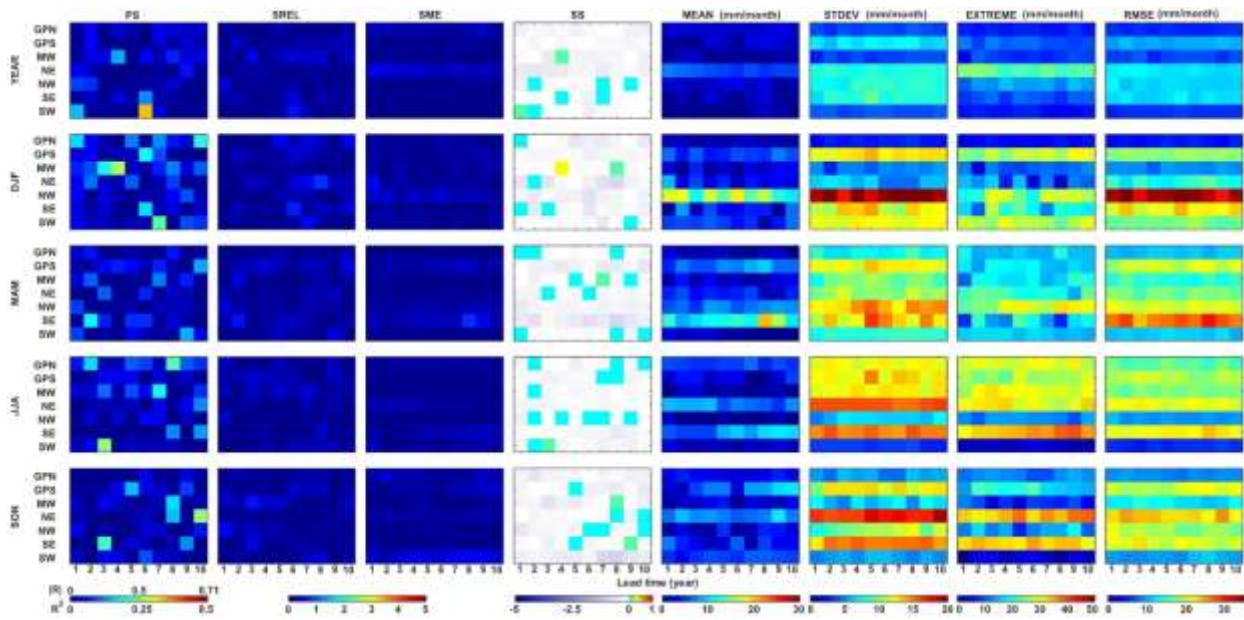
887



888

889 Figure 7: Same as Figure 4 but for the ensembles of LR based *statistically downscaled* GCM
 890 predictions.

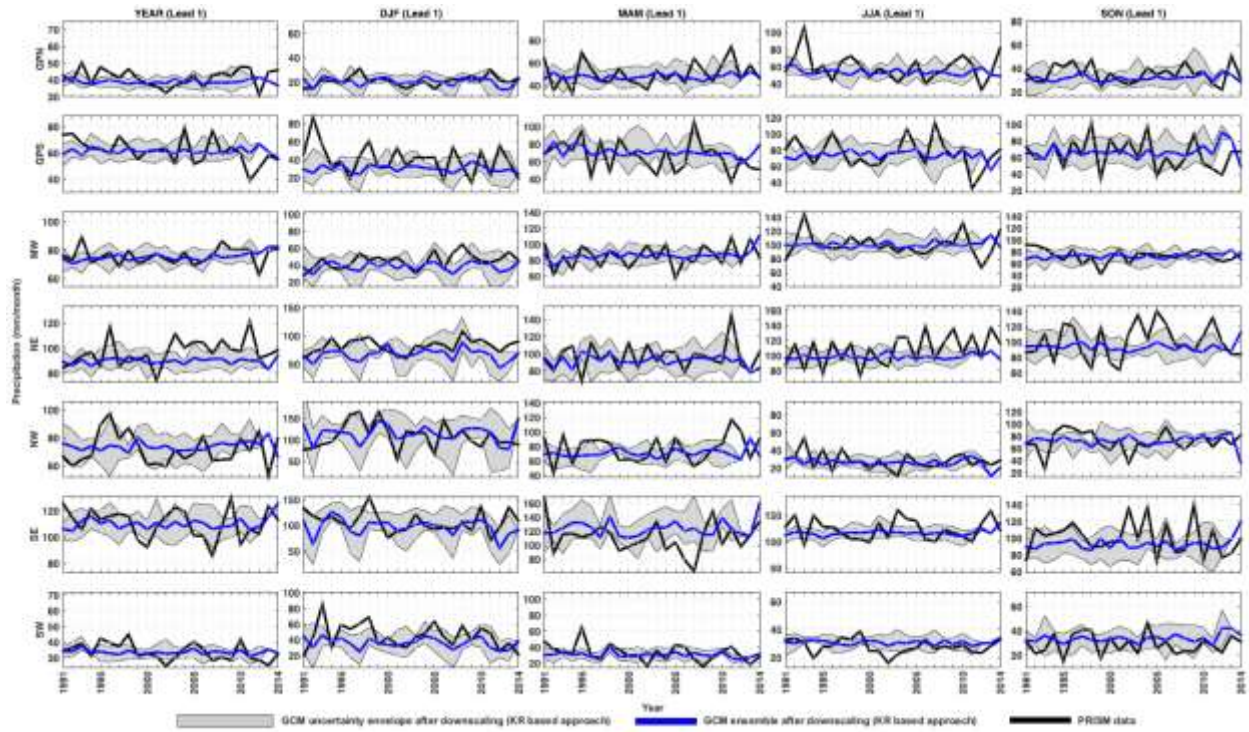
891



892

893 Figure 8: Same as Figure 3 but for seasonally and regionally averaged ensembles of KR based
 894 *statistically downscaled* GCM predictions.

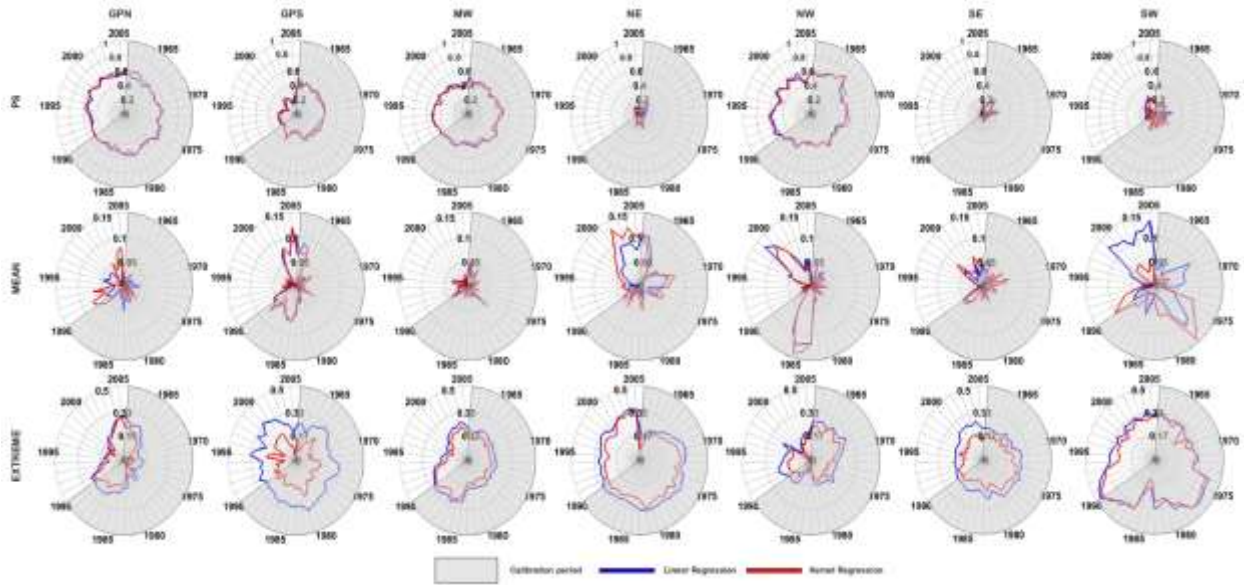
895



896

897 Figure 9: Same as Figure 4 but for the ensembles of KR based *statistically downscaled* GCM
 898 predictions.

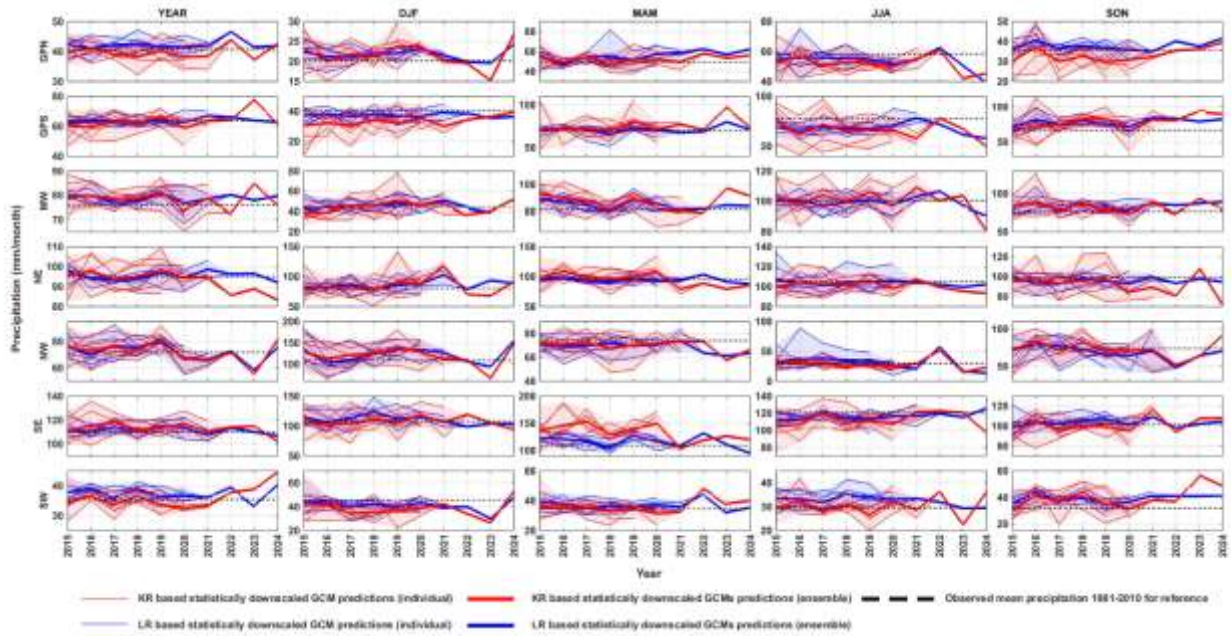
899



900

901 Figure 10: Radar plots comparing the skill between statistically downscaled precipitation skills
 902 (LR based, shown by blue color and KR based shown by red color) in the decadal framework.
 903 Each spoke represents the year of initialization. The gray region shows the skills for the years
 904 where year of initialization belongs to the calibration period (1961-1990).

905



906

907 Figure 11: Precipitation predictions for the near future decade 2015-2024. Seasonally and
 908 regionally averaged ensemble of LR based statistically downscaled precipitation data (thick blue
 909 line), surrounded by individual bias corrected GCM prediction trajectories (thin blue lines) and
 910 envelope (light blue shaded region) showing the uncertainty associated with it. Red lines/shaded
 911 region are the exact counterparts of the LR based statistically downscaled precipitation but
 912 obtained with KR based SD methodology. The black dashed line represents the 30-year mean
 913 (1981-2010) to be used as reference for comparing future predictions.

914

915

916

917

918

919

920

921

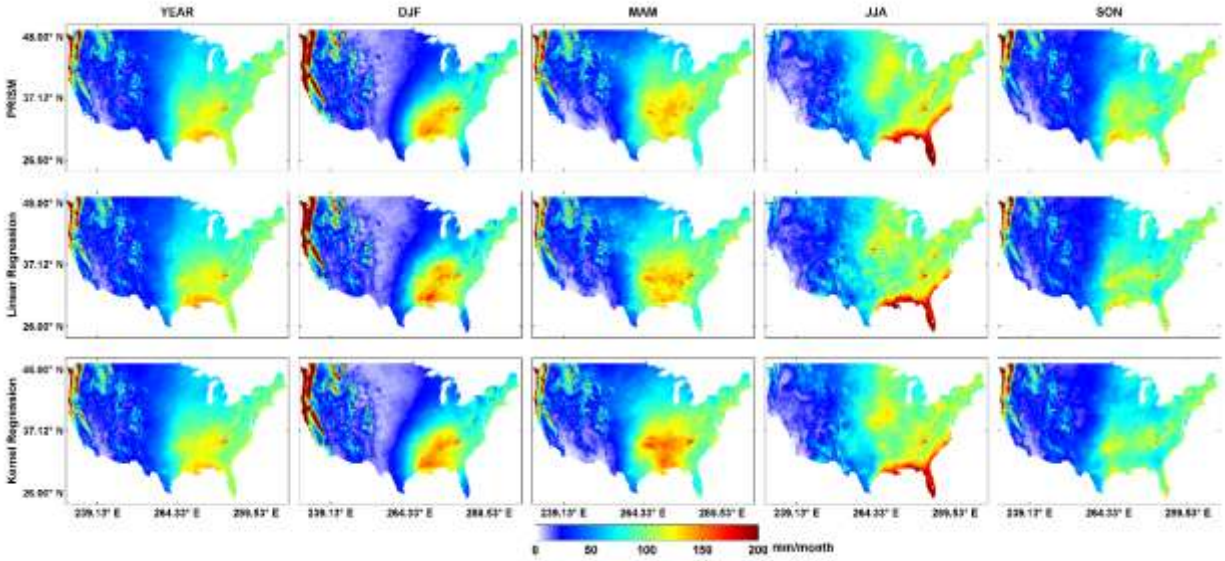
922

923

924

925

926



927

928

929 Figure 12: Comparison between PRISM mean precipitation (1991-2014) with statistically
 930 downscaled mean precipitation with linear and kernel regression based approach, applied to
 931 NCEP/NCAR reanalysis data predictors over different seasons. The methodologies are able to
 932 capture the orographic effects influencing spatial pattern of mean precipitation. The marked
 933 spatial variations in mean precipitation in PRISM (e.g., western United States) are captured by
 934 the two approaches.